A motion coordination formation control algorithm for fixed-wing unmanned aerial vehicles

Feng, Xuewei; Xie, Hongwei; Wang, Ximan; Wu, Changwei; Zhang, Xiaoliang

DOI
10.1109/CAC53003.2021.9728562

Publication date
2021

Document Version
Final published version

Published in
Proceeding of the China Automation Congress, CAC 2021

A motion coordination formation control algorithm for fixed-wing unmanned aerial vehicles

1st Xuewei Feng
College of software
Taiyuan University of Technology
Taiyuan, China
15235170935@163.com

2nd Hongwei Xie
College of software
Taiyuan University of Technology
Taiyuan, China
xiehongwei@tyut.edu.cn

3rd Ximan Wang
Delft Center for Systems and Control
TU Delft
Delft, The Netherlands
X.Wang-15@tudelft.nl

4th Changwei Wu
College of software
Taiyuan University of Technology
Taiyuan, China
1741456790@qq.com

5th Xiaoliang Zhang
College of software
Taiyuan University of Technology
Taiyuan, China
1131676434@qq.com

2021 China Automation Congress (CAC) | 978-1-6654-2647-3/21/$31.00 ©2021 IEEE | DOI: 10.1109/CAC53003.2021.9728562

***Abstract*—Formation control is the main subject of the coordination control of multi-agent system. The purpose of the control is to drive the system following a target position to keep some specific geometric structures by information exchange between agents. The formation geometry is described by a set of expected positions for all UAVs concerning the heading of the group. We try to display the relative position and attitudes on the formation control of numerous fixed-wing UAVs in this paper. And the behaviors of formation-hold about following are achieved by using the segment control based on unicycle-type by the heading rate of the vehicle are reviewed in this paper. Finally, the digital simulation implemented has validated the effectiveness of the proposed method.**

***Index Terms*—UAVs, formation, Unicycle Type Approach, the segment control**

I. Introduction

Unmanned Aerial Vehicles (UAV) or drones are known as powered flying vehicles without a human pilot onboard, that can be operated using a remote control or completely autonomously by an onboard computer and that can carry a payload. There are many different types of vehicles that are mainly Fixed-Wing, multi-copter, and Vertical Take-Off Landing(VTOL). The main advantage of fixed-wing UAVs is that its possible to fly by using a very less amount of energy or energy-free by using the airflow. So the fixed-wing UAVs serve in many applications, e.g. traffic control, payload transportation, pipeline inspection, road upkeep, dam supervision, forest fire search or view [1], search and rescue and so on. However, a single drone fails to execute any complex missions in some cases, for instance, large payload shipping, searching for something in a large area, etc. Researchers are more and more attracted by the cooperation of multiple UAVs because of these potential applications [2].

There exist various control strategies for a robot swarm for formation [3], such as behavior-based approaches, Virtual structure techniques and the leader tracking approach. The leader mobile robot moves along a predefined path while the followers sustain a desired distance and direction from the leader in the leader tracking approach [4]. The formation control between robots and fixed-wing UAVs has some similarities like collision avoidance and communication constraints. However, the UAV has a different dynamic and it needs to have a forward motion to generate the required lift to fly, thus stop-and-wait, stop-and-reverse, and instantaneous lateral motions are not possible. The frequently used methods of the structure of the UAVs include behavior-based, virtual structure, and the leader-follower methods in a comparable way. For the leader-follower approach, the leader vehicle plays a significant role as a reference in the group [4] [5] , while a virtual leader is widely adopted as the geometrical center of the formation in virtual-structure formation [6] [7] [8]. And the unicycle type controller, is a motion coordination formation control algorithm and a tracking controller used in robot obstacle avoidance. The output of the controller can achieve global asymptotic stability under some special constraints to track the reference trajectories [9].

In this paper, we introduce a separate control approach supported by the unicycle type tracking algorithm about the fixed-wing UAVs formation control, so that it can get close to and follow the leader and well to accomplish the formation flight. The main strategy used by the leader is simultaneously the vector fields (VFs) guidance control that provides the right desired heading to control of leader to arrive at the predesigned path in the horizontal plane introduced in [10] and [11].

The rest of this thesis is formulated as follows: Section II proposes some useful concepts including the problem formulation, kinematic models of the unicycle-type robot and leader-follower, and the tracking error dynamics. Then the definition of the algorithm for a fixed-wing aircraft model and the implementation of it in a virtual environment using the ROS with Gazebo Simulation as a physical simulator are elaborated description in Section III and IV respectively. Section V summarizes the thesis, eventually.

II. Preliminaries and Problem Formulation

Here, we recall some necessary useful concepts about the formations, and the unicycle type control strategy will be announced in this section, followed by the problem to be tackled.

A. Problem formulation

Consider a team of n flying fied-wing MAVs in $\mathbb{R}^2$. Denote $\boldsymbol{p_k} \in \mathbb{R}^2$ as the position of the kth UAV and $\boldsymbol{p} = [\boldsymbol{p_1}, \boldsymbol{p_2}, ..., \boldsymbol{p_n}] \in \mathbb{R}^{2\times n}$ as the corresponding configuration. And a distance, between a position $\boldsymbol{p_0} \in \mathbb{R}^2$ and a set $\mathcal{L} \subset \mathbb{R}^2$, is denoted by $\text{dist}(\boldsymbol{p_0}, \mathcal{L}) = inf\{||\boldsymbol{p} - \boldsymbol{p_0}|| : \boldsymbol{p} \in \mathcal{L}\}$. In addition, the distance between two nonempty sets $\mathcal{M}$ and $\mathcal{N}$ is $\text{dist}(\mathcal{M}, \mathcal{N}) = \text{dist}\ (\mathcal{M}, \mathcal{N}) = inf\{||m - n|| : m \in \mathcal{M}, n \in \mathcal{N}\}$.

We consider which the airspeed speed of leader can be regarded as constant V^l, has to follow a path $\mathcal{L} \subset \mathbb{R}^2$. Meanwhile, there exists n - 1 followers are following it and V_k^f describes the airspeed speed of kth follower. The desired states are that speeds of followers are $V_k^f \to V^l$, as $t \to +\infty$, the directions between V_k^f and V^l have kept the same direction. And the corresponding position between the leader and follower can form the expected shape. Therefore, this paper has to design a feedback control law for which the closed-loop signals can be bounded, follows

$$||\boldsymbol{p_k}(t) - \boldsymbol{p'_k}(t)|| \to \epsilon_1, ||V_k^f(t) - V^l(t)|| \to \epsilon_2, \quad \forall \epsilon_* \to 0, t \to +\infty \quad (1)$$

where $\boldsymbol{p'_k} = (\boldsymbol{x'_k}, \boldsymbol{y'_k})$ is the desired postion of kth follower in the inertial frame. $\boldsymbol{p_k}, \boldsymbol{p'_k}, V_k^f$ and V^l are all time variables in (1).

B. Kinematic model of the Unicycle-type mobile robot

In this paper, we consider which UAV flies at a constant altitude. According to [9] and [12], the kinematic model of a UAV can be given as follows:

$$\begin{aligned} \dot{x}_k &= V_k sin(\psi_k) \\ \dot{y}_k &= V_k cos(\psi_k) \\ \dot{\psi}_k &= \omega_k \end{aligned} \quad (2)$$

where $k \in \{l, f_i\}$, $i \in \{1, 2, ..., n-1\}$ and l represents the leader, f_i is the number of ith follower. As the define in the previous subsection, $x_k \in \mathbb{R}$ and $y_k \in \mathbb{R}$ are the coordinates of the kth UAV in the local east-north-up (enu) Cartesian coordinate system and ψ_k is its heading angle relative to the x-axis of the enu frame. V_k and ω_k are the airspeed speed and angular velocities. $(\dot{x}_k, \dot{y}_k)$ represents the x and y components of the linear velocities in the body frame for kth vehicle. The variables announced above are characterized in Fig. 1. The motion (2) should satisfy the nonholonomic constraint (3). Equation (4) shows the motion constraints of UAV about the airspeed speed and heading rate.

$$\dot{x}_k sin\psi_k = \dot{y}_k cos\psi_k \quad (3)$$

$$V_{min} \le V_k \le V_{max}, |\omega_k| \le \omega_{max} \quad (4)$$

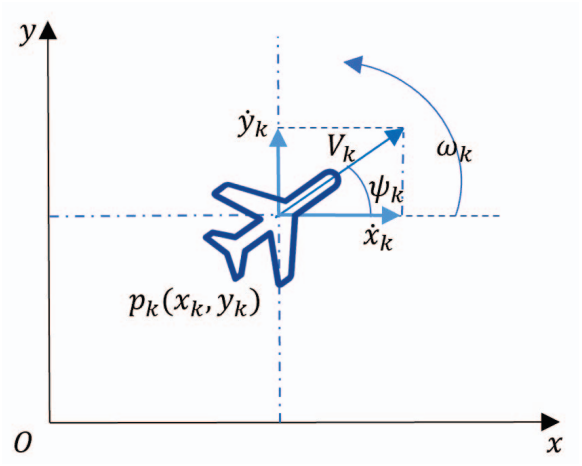

Fig. 1: A model of the fixed-wing vehicle which are used to analyze states of the model.

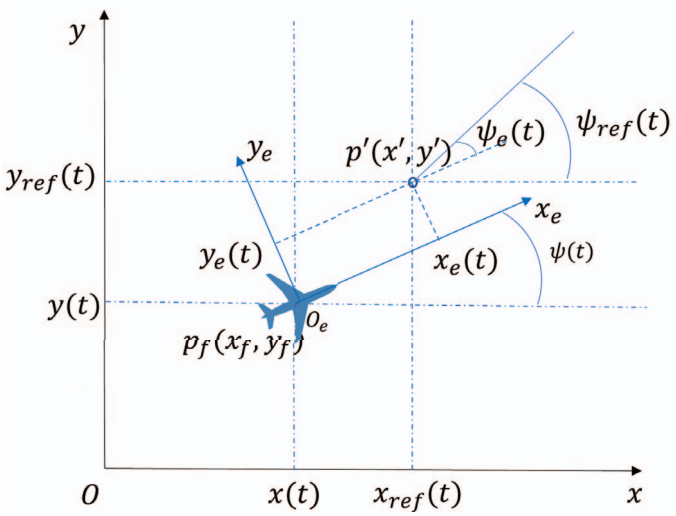

Fig. 2: The refered position $\boldsymbol{p'}(x', y')$ for the follower is a sum of the leader position plus $\boldsymbol{G}$ as shown in the figure. ψ_e is represented the angle-track error. x_e and y_e represent the cross-tracking error.

where V_{min}, V_{max} and ω_{max} are all positive constants.

In addition, we wish introduce some notations of the formation trajectory firstly. The formation trajectory can be expressed by $\boldsymbol{t_l}(t) = [x_l(t), y_l(t), \psi_l(t), v_l(t), \omega_l(t)]$, where $t \in [0, t_f]$ and l is leader number. The formation speed is the speed of the formation trajectory. Similarly, the heading rate of the formation trajectory is represented as the formation heading rate [12].

C. Kinematic model of Leader-Follower and Tracking Error Dynamics

The leader-follower formation model, called L-F Kinematic model, is shown in Fig. 2. The configuration is introduced by (2) which defined the simplified kinematic models for fixed-wing aircrafts suitable for the leader and the followers.

In this paper, we use the subscript f and l to represent each follower and leader instead of the subscript k. We solve the tracking problem by calculating ω_c and V_c such that the ψ_f converges to ψ_l, the cross-track error d converges to reaches zero asymptotically, and to maintain the prefined formation with the leader. In addition, the follower should also reach the same airspeed speed as the leader gradually, $V_f \to V_l$.

The desired position of the follower $\boldsymbol{p'}(x', y')$ at the current moment can be calculated according to the predefined $\boldsymbol{G}$ and the current position of the leader, firstly.

$$\boldsymbol{p'} = \begin{bmatrix} x' \\ y' \end{bmatrix} = \boldsymbol{WG} + \boldsymbol{p_l} \tag{5}$$

$$\boldsymbol{W} = \begin{bmatrix} cos(tan^{-1}(g_y/g_x) + \psi_l) \\ sin(tan^{-1}(g_y/g_x) + \psi_l) \end{bmatrix}^T, \boldsymbol{G} = [g_x, g_y]^T \tag{6}$$

where the $\boldsymbol{G}$ represents the position vector of the follower relative to the leader after the stable formation in the horizontal plane, which is used to specify a particular formation. Therefore, the position $\boldsymbol{p'}(x', y')$ is a target point that the follower needs to reach at the current time. And we consider tracking errors $\boldsymbol{E}$, time-dependent variables, represented in the coordinate frame of the body frame:

$$\begin{aligned} \boldsymbol{E}(t) &= \begin{bmatrix} x_e \\ y_e \\ \psi_e \end{bmatrix} = \begin{bmatrix} cos\psi_f & sin\psi_f & 0 \\ -sin\psi_f & cos\psi_f & 0 \\ 0 & 0 & 1 \end{bmatrix} \begin{bmatrix} x' - x_f \\ y' - y_f \\ \psi_l - \psi_f \end{bmatrix} \\ &= \begin{bmatrix} cos\psi_f(x' - x_f) + sin\psi_f(y' - y_f) \\ -sin\psi_f(x' - x_f) + cos\psi_f(y' - y_f) \\ \psi_l - \psi_f \end{bmatrix} \end{aligned} \tag{7}$$

The derivative of (7) yields the following expression:

$$\dot{\boldsymbol{E}}(t) = \begin{bmatrix} \dot{\psi}_f y_e - v_f + v_l cos\psi_e \\ -\dot{\psi}_f x_e + v_l sin\psi_e \\ \omega_l - \omega_f \end{bmatrix} \tag{8}$$

where the variables x_e and y_e are the representation of the error relative to the body coordinate system after the rotation of ψ_f in the east-north-up coordinate system. ψ_e is the heading error between the follower and leader.

III. DESCRIBE OF TRACKING CONTROLLER

Here, we will describe a controller to generate the desired ω_c and V_c for the follower to chase leader, which ensures global asymptotic stability of the error dynamics (8) according to the experiments in section IV. This will take into consideration the position of the leader plus a gap in (6) as the goal of the controller. Moreover, this target point is moving and the followers need to reach it under the controller and achieve stability while the leader is flying in several different path shapes lastly. Also, other data from the leader will be taken into consideration to build up the control solution.

A. Controller of the Angular Rate

In order that chasing the target point $\boldsymbol{p'}$ to achieve the purpose of the predefined formation trajectory $\boldsymbol{t_l}(t)$. We, firstly, should consider how to keep the flight direction of the follower and the distance vector direction from the local position to the goal point all the time and catching under a certain speed controller. Something else they need to be careful about which these variables involved are all functions of time-variant. Based on these problems above, we will exhibit the following control laws of heading rate which ensures global asymptotic stability of the tracking error dynamics:

$$\omega_{c1} = k_\omega(\psi_{ref} - tan^{-1}(\frac{\pi}{2} - \psi_{ref})) \tag{9}$$

$$\begin{aligned} \omega_{c2} = \omega_{ref} &- tan^{-1}(\frac{y_e}{k_y\sqrt{1 + (x_e)^2 + (y_e)^2}}) \\ &+ (\omega_{max} - |\omega_l| - k_v v_l)tanh(k_\psi \psi_e) \end{aligned} \tag{10}$$

where $k_\omega, k_y, k_\psi, k_v \in R_+$ are design parameters. The cross-tracking error d represents the straight-line distance between the follower and the desired target point $\boldsymbol{p'}$, and τ is a distance parameter used to segment and limit the scope of action of the controller.If e_ψ is greater than τ, the (9) would be activated. Otherwise, the (10) that is mainly introduced in this paper would be in motion. The $tanh(\cdot)$ whose value range is from -1 to 1 is the hyperbolic tangent function. And the expected angular velocity is a continuous uniformly bounded variable with the following constraints:

$$u = \begin{cases} -V_f^2/R_{\min} & \text{if } |u| > V_f^2/R_{\min} \text{ and } u < 0 \\ V_f^2/R_{\min} & \text{if } |u| > V_f^2/R_{\min} \text{ and } u > 0 \\ u & \text{otherwise} \end{cases} \tag{11}$$

where the lateral acceleration u, restricted to above formula, is equal to $V_f\omega_{c*}$, and $* \in \{1, 2\}$. $R_{\min}$ is the minimum turning radius of the airplane and can make sure you keep the airplane in balance and keep the turn coordinated.

B. Controller of the Speed

The controller of the angular rate can make sure that y_e in (8) will decrease to near zero, as time goes on. The error model only needs to consider x_e which was defined on the x-axis of the follower airframe axis now. Therefore, it is necessary to design a speed controller for contributing enough thrust to generate the desired velocity to decrease the x_e.

We can imagine the setpoint as a point in a 1D space moving at the same speed as the leader, the desired speed of the follower should be the same speed as the leader when the follower has reached the target point. If the follower is after the point, the expected airspeed speed will be lower than the airspeed speed of the point. And, if the follower is behind the point, it will have to keep a speed higher than the leader to reach the goal position. Given the considerations, we can define V_c:

$$V_c = k_s(|V_f - V_l|)x_e + V_l \tag{12}$$

where the variables x_e and ψ_e can be calculated by the (7). $|\cdot|$ represents the absolute value of a number. k_s is a proportional gain that defines how aggressive is the correction given errors x_e, and $k_s \in R_+$.

TABLE I:
Variables for the Formation Control

variable	Description
$\mathcal{R}$	rotation matrix from enu to vehicle frame
S_l	airspeed speed of the leader
τ	distance error threshold
ψ_l	the heading for the leader
ψ_f	the heading for the follower
ω_{max}	the maximal heading rate of the UAV
$\boldsymbol{G} = (g_x, g_y)$	gap value of the distance leader
$\boldsymbol{p_l} = (x_l, y_l)^T$	enu coordinates for the leader
$\boldsymbol{p_f} = (x_f, y_f)^T$	enu coordinates for the follower
$k_s, k_\omega, k_y, k_v, k_\psi$	convergence gains, positive number all

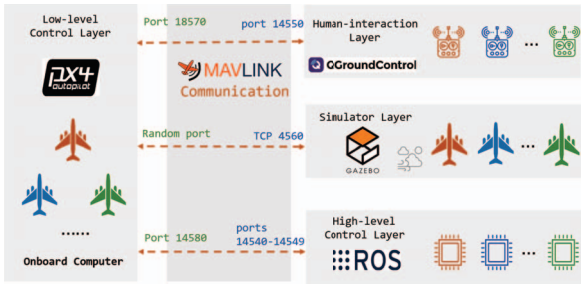

Fig. 3: A typical SITL simulation environment [13] for simulators.

C. Pseudocode of the Controllers

We make an outline of the formation controller algorithm and a complete list of the variables used for the algorithm which can be found in algorithm 1 and Table I. The primary idea is to make sure the position where the MAVs are in a horizontal plane and then command the desired heading rate and speed to result in a stable formation, defined in the beginning. The numerical simulations will be described in the next section.

Algorithm 1 Formation Control of Unicycle-type Algorithm(in the horizontal plane)

Input: $\boldsymbol{G}, S_l, \boldsymbol{p_f}, \boldsymbol{p_l}, \psi_l, \psi_f$

$\boldsymbol{p'} \leftarrow (cos(\epsilon + \psi_l)G + x_l, sin(\epsilon + \psi_l)G + y_l)$
$\boldsymbol{e} \leftarrow \boldsymbol{p'} - \boldsymbol{p_f}$
$\boldsymbol{E} \leftarrow \mathcal{R}\boldsymbol{e}$
$\psi_e \leftarrow \psi_l - \psi_f$
$d \leftarrow ||\boldsymbol{e}||$
if $d > \tau$ **then**
  $V_c \leftarrow k_s V_l$
  $\omega_{c1} = k_\omega(\psi_{ref} - tan^{-1}(\frac{\pi}{2} - \psi_{ref}))$
else
  $V_c \leftarrow k_s(|V_f - V_l|)x_e + V_l$
  $\omega_d^1 \leftarrow \omega_l - k_y tan^{-1}(y_e/d)$
  $\omega_d^2 \leftarrow (\omega_{max} - |\omega_l| - k_v V_l)tanh(k_\psi \psi_e)$
  $\omega_c \leftarrow \omega_d^1 + \omega_d^2$
end if

IV. Simulation

We will show a series of numerical simulation results over here to further illustrate the idea in the previous sections. We do the software-in-the-loop experiments in ROS, Gazebo, and PX4 platforms to simulate the wind and no wind environment by using the wind plugin of Gazebo to define the scenarios in straight, orbit, and lemniscate path, the relationship between these platforms can be shown in Fig. 3. And the main parameters of the wind plugin have been defined that are WindForceMax = 3.5, WindForceMean = 2.5, WindGuestMax = 10,WindGuestMean = 7, WindDirectionMean = 45^o. Because the lemniscate path is composed of straight-line and orbit paths, we select a straight-line path, orbit path, and lemniscate path to test the idea.

In this section, two UAVs were hired to formation, one is regarded as the formation leader and another is regarded as the follower. And the parameters obtained from tests are defined as $\boldsymbol{G} = (-10, -10)^T, k_s = 2, k_\omega = 1, k_y = 0.04, k_v = 0.11, k_\psi = 4, \tau = 30, \omega_{max} = 1.0472$. According to these, We will introduce simulations from each of these three aspects respectively.

A. Straight-line Path Simulation

In straight path, the leader is flying along the predetermined flight path in the lower left corner as a list of waypoints including (-300, -300), (-1000, -1000), (-1500, -1500) and (-3500, -3500). At this point, the follower begins to following from 45 degrees in the upper right, approximately 250m as shown in Fig. 4a and 5a. Fig. 5b and 5b shows the distance error from the local position to the desired position.

The leader plane is flying on a straight-line path, while the follower plane begins to chase at point (0, 0) nearly. And the formation trajectory is

$$\boldsymbol{t_l}(0) = [-178.80, -174.12, 3\pi/4, 14.60, 0.1425]$$

which the speed and heading rate of formation trajectory are 14.60 meters per second and 0.1425 radians per second, respectively. Fig. 4 shows the chasing path and error analysis images in no wind environment. Fig. 5 describes the same meaning in windy conditions.

In the beginning, because the distance error is much greater than the threshold τ, the speed controller will calculate a full throttle to chase the point. On the way, the mean velocity of the leader is 16.85 meters per second, and the maximum velocity of the follower can reach 21 meters per second. With a large speed difference, the distance error is increasingly smaller under the action of time. In the case of no wind, it enters the threshold at about 150 seconds. Under controllers in (10) and (12), the distance d and the velocity deviation can be stabilized within $(0, 3)$ meters and $[-1, 1]$ meters per second respectively. With the passage of time and the action of piecewise controllers, the error offset is gradually shortened. Finally, they can be stabilized around zero that the displacement error fluctuates less than 5 meters as shown in Fig. 4b and Fig. 5b, and the maximum velocity error can be

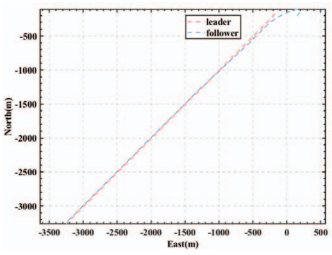

(a) SITL Straight: No wind

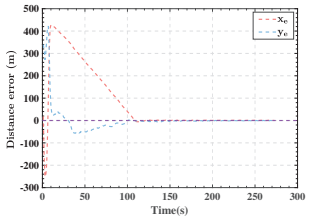

(b) Distance error in no wind

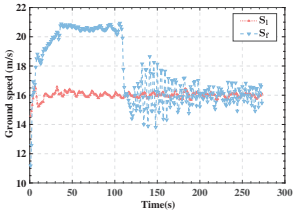

(c) airspeed speed in no wind

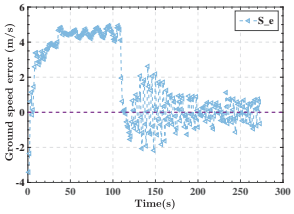

(d) Speeds error in no wind

Fig. 4: The simulation of the straight in no wind environment including the path, distance error of x-axis and y-axis, airspeed speeds of leader and follower, and their difference diagrams.

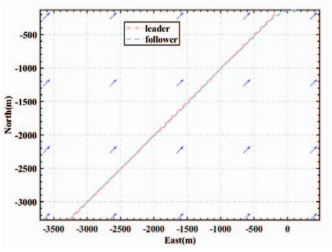

(a) SITL Straight: wind

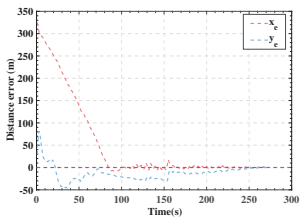

(b) Distance error in wind

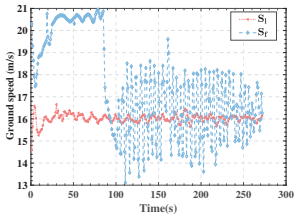

(c) airspeed speeds in wind

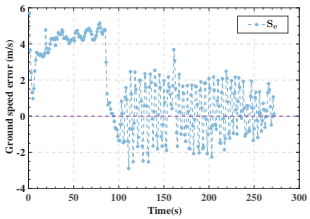

(d) Speeds error in wind

Fig. 5: The simulation of the straight in wind environment including the path, distance error of x-axis and y-axis, airspeed speeds of leader and follower, and their difference diagrams.

stabilized at [-2, 2] meters per second as shown in Fig. 4d and Fig. 5d. Because of the disturbance of wind, it takes longer to enter the inside about 200 seconds.

B. Orbit Path Simulation

In the orbit path, we consider that make the leader fly in which the loiter radius is 600 meters, and the center of the circle is (0,0). When the leader is flying at (498.72, -454.19), the follower starts the algorithm at (36.08, -54.25). And the

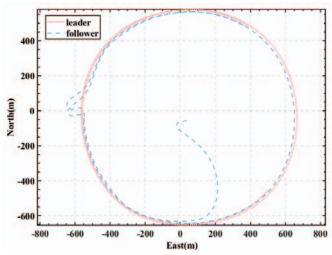

(a) SITL Orbit: No wind

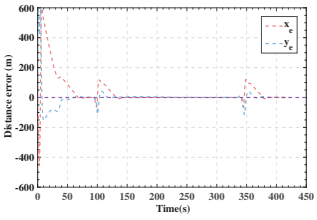

(b) Distance error in no wind

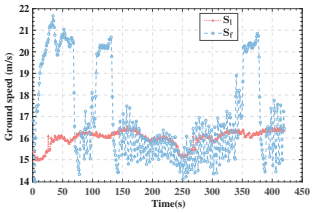

(c) SITL Orbit: No wind

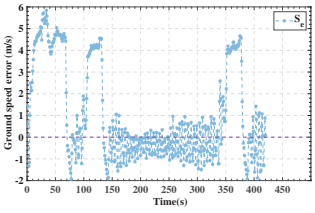

(d) Distance error in wind

Fig. 6: The simulation of the orbit in no wind environment including the path, distance error of x-axis and y-axis, airspeed speeds of leader and follower, and their difference diagrams.

formation trajectory is

$$\boldsymbol{t_l}(0) = [498.72, -454.19, 3\pi/4, 15.37, 0.2456]]$$

which the speed and heading rate of formation trajectory are 15.37 meters per second and 0.2456] radians per second, respectively. Due to $\boldsymbol{G}$, the follower's radius is less than 600 meters and the roll angle of the follower is much larger than that of the leader. This condition also puts forward high requirements for speed control to stabilize the formation after overtaking. The leader's airspeed speed can be stabilized around 16 meters per second under the right throttle. The simulation results of the two scenarios have shown in Fig. 6 and Fig. 7. In the beginning, under two types of controllers, the follower catches up with the goal point at high speed. In the case of no wind, the follower suddenly lost control after 100 seconds and 350 seconds resulting in the direction angle being uncontrolled. And the position deviations in both the x-axis and y-axis were greatly changed. In the case of wind, the follower also lost control when it received the same leader data after 100 seconds. Luckily, under the controller, it was all corrected. Ultimately, the x_e and y_e can be converged to zero meters, and the S_e is around [-2,2] meters per second in Figure 4d and 5d.

C. Lemniscate Path Simulation

In the lemniscate path, we run a leader and a follower in formation fly in both no wind and wind environment and observe how to keep the predefined formation as well. The lemniscate path is sent to the leader as a list of waypoints including (300, 300), (1000, -1000), (-300, 300) and (-1000, -1000). And the leader can execute them one by one circularly.

If the relationship between the leader position and the executing waypoint is satisfied with the fillets algorithm condition

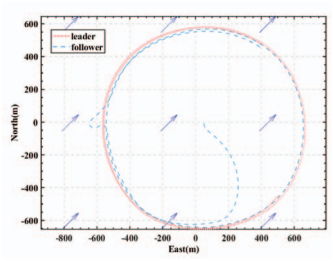

(a) SITL Orbit: wind

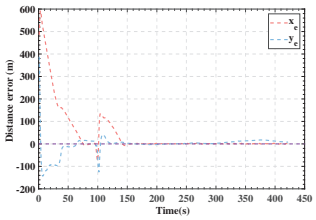

(b) Distance error in wind

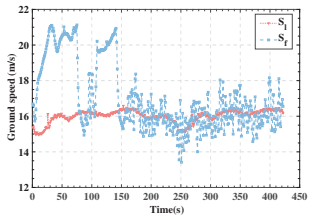

(c) airspeed speeds in wind

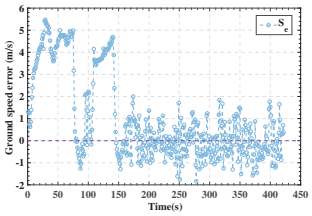

(d) Speeds error in wind

Fig. 7: The simulation of the orbit in the wind environment including the path, distance error of x-axis and y-axis, airspeed speeds of leader and follower, and their difference diagrams.

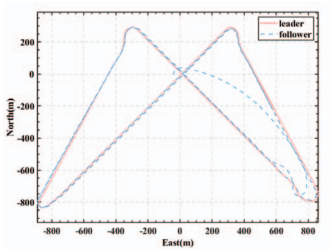

(a) SITL Mix: No wind

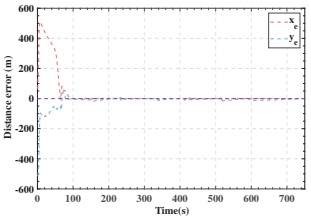

(b) Distance error in no wind

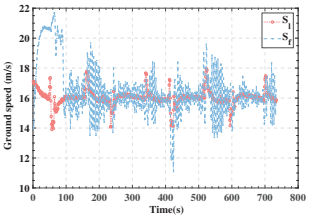

(c) airspeed speeds in no wind

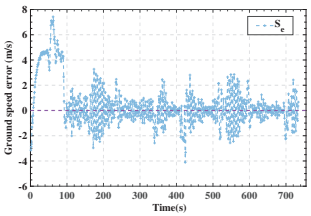

(d) Speeds error in no wind

Fig. 8: The simulation of the lemniscate in no wind environment including the path, distance error of x-axis and y-axis, airspeed speeds of leader and follower, and their difference diagrams.

introduced in [14], the leader will change the waypoint and choose the path following control strategies to the next in the waypoint list. The simulation results of the two scenarios have shown in Fig. 8 and Fig. 9.

The initial position of the follower is (-42.3, -5.7) when the algorithm is enabled. And the formation trajectory is

$$\boldsymbol{t_l}(0) = [487.9, -36.1, \pi/4, 17.11, 0.3123]$$

which the speed and heading rate of formation trajectory are 17.11 meters per second and 0.3123 radians per second. Fig. 8 shows the chasing path and error analysis images in no wind environment. Fig. 9 describes the same meaning in windy conditions. With the passage of time and the action of piecewise controllers, the offset is gradually shortened.

At first, the follower is chasing the goal point under full throttle at an average speed of 21 meters per second. As time goes on, the offsets are narrowing rapidly. Reaching within the threshold, it spent about 100 seconds. When the leader starts to change waypoints, the x_e and y_e are increasing. And then the controller comes in and corrects the deviation. Therefore, the jagged shape appeared in 8b and 9b. The remaining graphs show the velocity change curve of leader-follower.

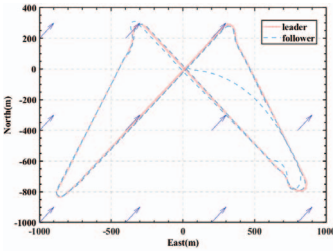

(a) SITL Mix: wind

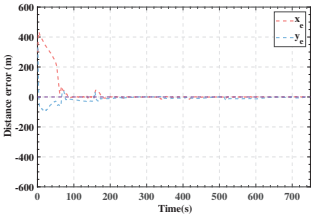

(b) Distance error in wind

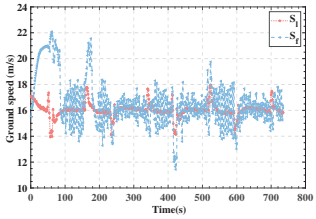

(c) airspeed speeds in wind

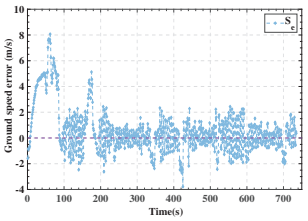

(d) Speeds error in wind

Fig. 9: The simulation of the lemniscate in wind environment including the path, distance error of x-axis and y-axis, airspeed speeds of leader and follower, and their difference diagrams.

V. CONCLUSIONS

This paper proposed a new formation control strategy by combining unicycle type control idea and segmented control idea to search the UAV formation flight. From the outcome of Software-in-the-Loop experiments about three kinds of trajectories, it is possible to conclude that the blueprint can be well tested in the wind or no wind environment.

Although the analysis has not considered a different type of platforms, like Hardware-in-the-Loop experiments and realistic platforms, the findings are of direct practical relevance.

Future work will involve applying the idea of UT to the path following algorithm for the leader in a horizontal direction with the constant altitude. We also expect to research a three-dimension path-following algorithm about this idea and analyze it under a variety of circumstances.

REFERENCES

[1] M. Şahin and M. T. Yıldırım, "Application of a fixed-wing unmanned aerial vehicle (uav) in reforestation of lebanon cedar (cedrus libani a. rich)." 6th Ankara International Aerospace Conference,

AIAC 2011 (14 - 16 Eylül 2011), 2011. [Online]. Available: http://aiac.ae.metu.edu.tr/paper.php?No=AIAC-2011-073

[2] Z. Hou, W. Wang, G. Zhang, and C. Han, "A survey on the formation control of multiple quadrotors," in *2017 14th International Conference on Ubiquitous Robots and Ambient Intelligence (URAI)*, 2017, pp. 219–225.

[3] H. Zhi-Wei, L. Jia-Hong, C. Ling, and W. Bing, "Survey on the formation control of multi-agent system," in *Proceedings of the 31st Chinese Control Conference*, 2012, pp. 6092–6098.

[4] A. Alfaro and A. Morán, "Leader-follower formation control of non-holonomic mobile robots," in *2020 IEEE ANDESCON*, 2020, pp. 1–6.

[5] W. Yuan, Q. Chen, Z. Hou, and Y. Li, "Multi-uavs formation flight control based on leader-follower pattern," in *2017 36th Chinese Control Conference (CCC)*, 2017, pp. 1276–1281.

[6] J. Li, D. Xue, and J. Zhang, "Multi-uuv formation coordination control based on combination of virtual structure and leader," in *2018 IEEE International Conference on Mechatronics and Automation (ICMA)*, 2018, pp. 1574–1579.

[7] B. Cong, X. Liu, and Z. Chen, "Attitude coordination of deep space formation flying via virtual structure," in *Proceedings of the 29th Chinese Control Conference*, 2010, pp. 3810–3815.

[8] C. B. Low, "A dynamic virtual structure formation control for fixed-wing uavs," in *2011 9th IEEE International Conference on Control and Automation (ICCA)*, 2011, pp. 627–632.

[9] D. Kostić, S. Adinandra, J. Caarls, N. van de Wouw, and H. Nijmeijer, "Collision-free tracking control of unicycle mobile robots," in *Proceedings of the 48h IEEE Conference on Decision and Control (CDC) held jointly with 2009 28th Chinese Control Conference*, 2009, pp. 5667–5672.

[10] D. R. Nelson, D. B. Barber, T. W. McLain, and R. W. Beard, "Vector field path following for miniature air vehicles," *IEEE Transactions on Robotics*, vol. 23, no. 3, pp. 519–529, 2007.

[11] D. Nelson, D. Barber, T. McLain, and R. Beard, "Vector field path following for miniature air vehicles," *IEEE Transactions on Robotics*, vol. 23, no. 3, pp. 519–529, 2007.

[12] Y. Wang, M. Shan, and D. Wang, "Motion capability analysis for multiple fixed-wing uav formations with speed and heading rate constraints," *IEEE Transactions on Control of Network Systems*, vol. 7, no. 2, pp. 977–989, 2020.

[13] Sitl simulation environment. [Online]. Available: https://docs.px4.io/master/en/simulation/#sitl-simulation-environment

[14] R. W. Beard and T. W. McLain, *Small Unmanned Aircraft: Theory and Practice*. Princeton University Press, 2012.